

Design, Modeling and Control of a Hopping Robot

H. Rad, P. Gregorio and M. Buehler
Department of Mechanical Engineering
McGill Research Center for Intelligent Machines
McGill University, 817 Sherbrooke St. W.
Montreal, Quebec, Canada, H3A 2K6

Abstract

We report progress towards model based, dynamically stable legged locomotion with energy efficient, electrically actuated robots. We present the mechanical design of a prismatic robot leg which is optimized for electrical actuation. A dynamical model of the robot and the actuator as well as the interaction with ground is derived and validated by demonstrating close correspondence between simulations and experiments. A new continuous, and exactly implementable open loop torque control algorithm is introduced which stabilizes a limit cycle of the underlying fourth order intermittent robot/actuator/environment dynamics.

1 Introduction

Dynamically stable legged robots promise to be the mobile platform of choice compared to wheeled systems when it comes to mobility, versatility, speed, in all but the special cases where a continuous and smooth path of support is provided. However, before legged robots become practical, strong stability properties and autonomous operation are essential. In order to achieve these goals, two key issues which have not been addressed adequately in the past research on dynamically stable legged robots, electric actuation and model based control, are considered here.

First, we focus on electrical actuation, instead of hydraulics, as a clean, safe and cheap technology, suitable for indoor use and autonomous robots. It

will become clear in this report that replacing the hydraulic actuators on existing robots with electric motors is not a straight forward engineering issue. Since electric motors' torque/mass ratio is far from that of hydraulic actuators, robot design and control will be fundamentally affected and pose challenging research problems. For example, the actuation strategy of applying a step length change at maximum leg compression for maintaining a constant vertical body oscillation might be a reasonable strategy for powerful hydraulic actuators, but it should be clear that such an approach is no longer advisable with electric actuators. We have verified in simulations and experiments that indeed stable operation can no longer be achieved and propose a new stabilizing continuous controller with an average power consumption of only 80W.

Second, model based control with verified dynamic models of robot, dynamic interaction with the ground and the actuators themselves is mandatory if predictable performance is desired. This is especially crucial with electric actuators models which impose considerable operational limits. In addition, there exists currently a gulf between experimental and theoretical research in this field. Due to the lack of supporting experimental work, and due to insufficient modeling efforts, much of the recent analytical literature reviewed below operates in a vacuum; it is not clear which model simplifications, and actuator models are valid, and which analytical methods and results are meaningful in practice. The benefits of empirically relevant analytical work are considerable. It could lead to new

and better control laws, a formal procedure for gain selection to improve stability, in general a better understanding of the complicated dynamics of legged robots, and in the future, certainly, better guidelines for robot design.

Our work has been strongly motivated and inspired by past research in this field, primarily by Marc Raibert [12] who has led the field of dynamically stable legged locomotion during the past decade. He built a variety of running robots, starting with a planar one-legged machine [11], followed by a 3D one-legged, a two-legged planar robot, and a four-legged quadruped. His latest robots include a 3D two-legged robot, where each leg has four actuated degrees of freedom. Except for the first one-legged planar hopper, which was pneumatically actuated, his subsequent designs are actuated by powerful hydraulic actuators and rely on pneumatics for the leg spring only. This permitted Raibert to focus on robot design and control without being limited significantly by actuator constraints. The strategy was eminently successful and he built many different running robots based on almost standardized custom parts. It is important to realize that all of his robots are controlled by some derivative of the tri-partitioned decoupled control developed for the original one-legged planar hopper [12]. Most fundamental design and control concepts can be motivated by and tested on such a robot, and generalized to more complicated robots. V. Papantoniou [9] has followed a similar avenue. He has built a planar hopper actuated by two electric motors and using a derivative of Raibert’s controller. He employs a clutch which engages the spinning motor at maximum leg compression to maximize energy transfer to the leg. To make this approach work, the stance time needed to be increased considerably to $470ms$.

There is a growing literature on stability results for vertical hopping robots motivated by Raibert’s robots and based on various simplifying assumptions about robot dynamics, actuator models or control laws. Koditschek and Buehler [6] modeled and analyzed the stability of simplified versions of Raibert’s original pneumatically actuated hopping robot relying on unimodal return map theory. Vakakis and Burdick [13] have studied numerically the bifurcation phenomena of a similar model. Lap-

shin [7] provides a global stability proof for a model of Raibert’s vertical hopper with a linear spring, actuated by a step length change. Li and He [8] and Hmam [3] have recently analyzed the stability of simplified two legged models (two coupled vertical hoppers), based on actuator models which exert a force in parallel to the leg spring.

The paper is organized as follows. Section 2 discusses the mechanical design issues relevant to our robot design. A complete dynamical model is developed in Section 3. In Section 4 the control problem is formulated and a solution is presented in Section 5. In Section 6 we verify the model by recourse to experiments.

2 Leg Design

Since our work is motivated by Marc Raibert’s experimental success, which was strongly founded on his first planar one legged hopper, and since there exists a growing literature on stabilizing controllers for its simple model, we decided to follow the same basic design – a ‘polar’ design which consists of a prismatic leg connected to a body via a revolute joint. For the present research, we will only describe the leg itself and its actuation to achieve a constant hopping height.

Our choice of electric actuators imposes great (self imposed) restrictions in terms of available power and torque. Human muscle has a maximum power density of about $100W/kg$ (for a comparison of human muscle with other contractile materials see [5]), which is readily achievable with today’s “fractional horsepower” electric motors. These can attain peak power/mass ratios of up to $1kW/kg$ [1]! Nevertheless, performance comparable to muscles remains elusive. The reason is that muscles are “direct drive” actuators – they can develop their maximum force and power at the low speeds needed to drive the biological joints directly. Small motors, with a mass of about $1kg$, on the other hand, are severely torque limited, and the peak power is achieved only at high speeds ($5000-10,000$ RPM). Peak torque/mass ratios of $6Nm/kg$ are only reached by large direct drive motors whose intricate geometry (at present) cannot be scaled down to small motors [4]. This calls for a speed reducer

(gear) in order to match the high torque–low velocity requirements of biological/robotic joint motion to the available low torque–high velocity of small motors.

This has two main consequences: First, virtually all large gear reducing mechanisms introduce additional dynamics which cannot be ignored. A considerable fraction of the motor power can be consumed for merely accelerating gear inertia. Second, most high gear ratio mechanisms introduce significant loss of driving torque, up to 61% for a high quality three stage planetary gear head for a gear ratio range of 80 to 200 [1]. This precludes the use of fractional horsepower motors as direct drive force controlled actuators in legged robots in an analogous fashion to muscles. In addition, we need to convert the rotary motion of the motor into linear motion suitable for our prismatic leg (Figure 1). The only practical transmission that provides us both with revolute-to-linear motion translation and high efficiency ($\eta \leq 95\%$) is a ball screw.

Preliminary simulations pointed out that the main design challenge was to maximize the energy added during the short stance phase. In our case, the complete motor – ball screw – spring system must be optimized to this effect at some nominal operating point. Unfortunately, there are many practical considerations, which stand in the way of formulating and solving a standard optimization problem. For example, the stance time can be increased by lowering the spring constant. However, this increases the actuator travel during stance. This in turn requires a longer ball screw (only available at discrete lengths), which increases its moment of inertia (subject to catalog tables), which actually *limits* the energy added. In addition there is only a finite number of choices for suitable motors and ball screw lengths and leads. This results in a highly nonlinear and complex optimization problem. To simplify this task, we also discretized the number of available spring constants, and performed an exhaustive (computer) search: The components to maximize the added stance energy (approx. 10 J) were determined as an 80W brushed DC motor (Maxon, 1.3 kg), a 5mm/rev ball screw (RHP) and a 4kN/m spring (custom). The component selection is far from intuitive since the robot – actuator

is a fourth order dynamical system. For example, a higher power (100W), lower mass (0.3 kg) brushless motor fared far worse due to the smaller torque at low speed; the velocities where high power is available are never attained during the 0.1s stance time!

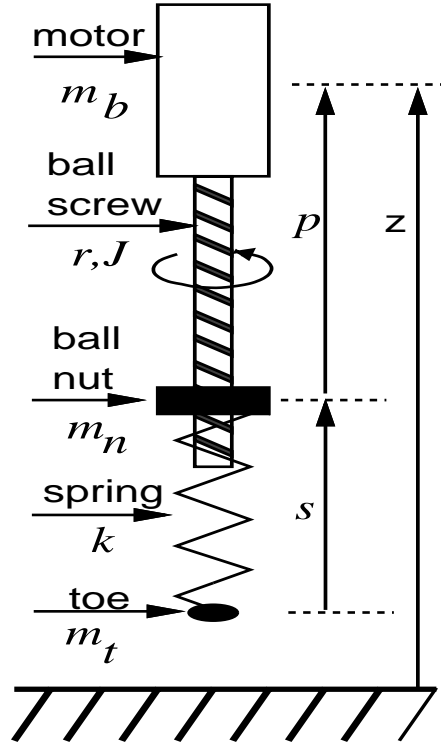


Figure 1: Hopper Model

With the main components selected, the remainder of the leg is designed for low mass and simplicity, and is shown in Figure 12. Starting at the top, the motor (with encoder) is coupled to the ball screw, whose moving nut attaches to the upper end of the compression spring. This motor – ball screw system constitutes our linear actuator with length p , as shown in Figure 1. The lower end of the spring is connected to the lower leg, an aluminum tube sliding in the upper leg tube on plastic sliders. We measure actuator length and body height via optical encoders and the leg length during stance via a linear potentiometer. Body height, forward travel and pitch are measured with respect to a planarizer mechanism, which keeps the robot restricted to a vertical plane. Currently, only the vertical travel is enabled.

3 Modeling

In the sequel the equations of motion for the hopper will be derived for two regions of phase space – stance phase, when the leg is in contact with the ground, and flight phase. The subscripts S and F denote stance and flight phase respectively. In addition, impulsive energy transfers are considered during touchdown and liftoff. The superscripts - and + denote variables just before and just after these instances. For conciseness, $m_{bn} = m_b + m_n$ and $m_{bnt} = m_b + m_n + m_t$. For a thorough treatment of ball screw dynamics and selection, see [10]. Table 1 provides a listing of all model parameters and experimental values.

z		Body Height
p		Actuator Length
τ		Motor Torque
θ		Motor Angle, $\theta = p/r$
s		Spring Length
m_b	9.5kg	Upper Leg Mass
m_n	0.25kg	Ball Nut Mass
m_t	0.5kg	Toe Mass
κ	4000N/m	Spring Constant
F_p	5.0N	Leg Dry Friction
F_z	1.5N	Planarizer Dry Friction
F_a	0N	Ball Screw Dry Friction
c	5.5Ns/m	Spring Viscous Friction
$\hat{\tau}$	1.78Nm	Stall Torque
$\hat{\omega}$	2800RPM	Max. Speed
η	0.95	Ball Screw Efficiency
s_0	0.608m	Spring Rest Length
l_0	0.595m	Maximum Leg Length
J	$2.7 \cdot 10^{-4} \text{kgm}^2$	Motor Inertia
α	0.34kgm	$J/r^2 + m_n$
μ	0.05	m_t/m_{bnt}

Table 1: Nomenclature; Note: m_b includes 5kg of bar bells to represent the future upper body mass.

3.1 Robot–Environment Model

3.1.1 Touchdown

Touchdown occurs when $z(t_{td}) = l_0$ and $\dot{z}(t_{td}) < 0$. At this instant the body velocity remains un-

changed,

$$\dot{z}^+ = \dot{z}^- = \dot{z}_{td}$$

but the kinetic energy of the unsprung mass m_t (the mass of the toe, the lower leg tube, and in practice a fraction of the spring mass itself), is dissipated. This energy loss can be expressed as a fraction of the robot’s kinetic energy just before touchdown,

$$\Delta E_{td} = \frac{1}{2} m_t \dot{z}_{td}^2 = \mu E_{kin,td}^-.$$

At a nominal touchdown velocity of $-2m/s$ this amounts to 1J for our robot.

3.1.2 Stance

The stance model is derived using the Lagrangian $L = T - V$, based on the generalized coordinates z and p . The total kinetic energy is given by

$$T_S = \frac{1}{2} J (\dot{p}/r)^2 + \frac{1}{2} m_b \dot{z}^2 + \frac{1}{2} m_n (\dot{z} - \dot{p})^2$$

where $p = r\theta$ is the kinematic ball screw relationship between motor angle θ and ball nut travel p . The potential energy is given by

$$V_S = m_b g z + m_n g (z - p) + \frac{1}{2} k (s_0 - z + p)^2.$$

The generalized nonconservative forces Q_z, Q_p consist of actuator torque, dry friction for the sliding parts and viscous friction for the spring losses. Using the virtual work principle we obtain

$$\begin{aligned} Q_z &= c(\dot{p} - \dot{z}) - f_{fS}, \\ Q_p &= \eta\tau/r - c(\dot{p} - \dot{z}) - f_a, \end{aligned}$$

where

$$\begin{aligned} f_{fS} &= (F_p + F_z) \text{sgn}(\dot{z}) \\ f_a &= F_n \text{sgn}(\dot{p}). \end{aligned}$$

The term F_p is due to friction between upper and lower leg and occurs only during stance phase. The F_z term is introduced from our planarizer mechanism, and is always present. F_n results from ball nut motion.

Following the Lagrangian formulation, we can now obtain the robot stance equations of motion,

$$\begin{bmatrix} \ddot{z} \\ \ddot{p} \end{bmatrix} = \mathbf{K}_S \begin{bmatrix} -m_{bn}g + f_{sS} - f_{fS} \\ m_n g + \eta\tau/r - f_{sS} - f_a \end{bmatrix},$$

with

$$\begin{aligned}\mathbf{K}_S &= 1/\beta_S \begin{bmatrix} \alpha & m_n \\ m_n & m_{bn} \end{bmatrix} \\ \beta_S &= m_{bn}\alpha - m_n^2 \\ f_{sS} &= \kappa(s_0 - z + p) + c(\dot{p} - \dot{z}).\end{aligned}$$

Representing this fourth order system in state space form we obtain

$$\dot{\mathbf{x}} = \mathbf{A}_S \mathbf{x} + \mathbf{b}_S \tau + \mathbf{e}_S(\mathbf{x}) \quad (1)$$

with

$$\mathbf{A}_S = \begin{bmatrix} 0 & 1 & 0 & 0 \\ -\kappa \frac{J}{\beta_S r^2} & -c \frac{J}{\beta_S r^2} & \kappa \frac{J}{\beta_S r^2} & c \frac{J}{\beta_S r^2} \\ 0 & 0 & 0 & 1 \\ \kappa \frac{m_b}{\beta_S} & c \frac{m_b}{\beta_S} & -\kappa \frac{m_b}{\beta_S} & -c \frac{m_b}{\beta_S} \end{bmatrix},$$

$$\mathbf{x} = \begin{bmatrix} z \\ \dot{z} \\ p \\ \dot{p} \end{bmatrix}, \quad \mathbf{b}_S = \frac{\eta}{\beta_S r} \begin{bmatrix} 0 \\ m_n \\ 0 \\ m_{bn} \end{bmatrix},$$

$$\mathbf{e}_S(\mathbf{x}) = \frac{1}{\beta_S} \begin{bmatrix} 0 \\ \alpha(\kappa s_0 - m_{bn}g - f_{fS}) + \\ m_n(m_n g - \kappa s_0 - f_a) \\ 0 \\ -m_n f_{fS} - m_b \kappa s_0 - m_{bn} f_a \end{bmatrix}.$$

3.1.3 Liftoff

When the leg is fully extended, $z(t_{l_0}) = l_0$ and $\dot{z}(t_{l_0}) > 0$ liftoff occurs. At this instant, due to conservation of linear momentum,

$$m_{bn} \dot{z}^- = m_{bnt} \dot{z}^+, \quad \dot{z}^+ = \frac{m_{bn}}{m_{bnt}} \dot{z}^- = (1 - \mu) \dot{z}^-.$$

If we assume that the actuator is at rest at liftoff, we can express again the energy loss at liftoff as a fraction of the kinetic energy just before liftoff,

$$\Delta E_{l_0} = \mu E_{kin, l_0}^-.$$

Again, we loose the same amount of energy as at touchdown, namely approximately $1J$ for a nominal liftoff velocity of $2m/s$.

3.1.4 Flight

The flight model is derived in an analogous fashion as the stance model. Now we have

$$T_F = \frac{1}{2} J (\dot{p}/r)^2 + \frac{1}{2} m_{bt} \dot{z}^2 + \frac{1}{2} m_n (\dot{z} - \dot{p})^2$$

and

$$V_F = m_{bt} g z + m_n g (z - p) + \frac{1}{2} k (s_0 - l_0 + p)^2.$$

The generalized nonconservative forces are now

$$\begin{aligned}Q_z &= -f_{fF} = -F_z \operatorname{sgn}(\dot{z}), \\ Q_p &= \eta \tau / r - c \dot{p} - f_a.\end{aligned}$$

Following the Lagrangian formulation, we can now obtain the robot flight equations of motion:

$$\begin{bmatrix} \ddot{z} \\ \ddot{p} \end{bmatrix} = \mathbf{K}_F \begin{bmatrix} -m_{bnt}g - f_{fF} \\ m_n g + \eta \tau / r - f_{sF} - f_a \end{bmatrix},$$

with

$$\begin{aligned}\mathbf{K}_F &= 1/\beta_F \begin{bmatrix} \alpha & m_n \\ m_n & m_{bnt} \end{bmatrix} \\ \beta_F &= m_{bnt}\alpha - m_n^2 \\ f_{sF} &= \kappa(s_0 - l_0 + p) + c \dot{p}.\end{aligned}$$

In state space form we obtain

$$\dot{\mathbf{x}} = \mathbf{A}_F \mathbf{x} + \mathbf{b}_F \tau + \mathbf{e}_F(\mathbf{x}) \quad (2)$$

with

$$\mathbf{A}_F = \begin{bmatrix} 0 & 1 & 0 & 0 \\ 0 & 0 & -\kappa \frac{m_n}{\beta_F} & -c \frac{m_n}{\beta_F} \\ 0 & 0 & 0 & 1 \\ 0 & 0 & -\kappa \frac{m_{bnt}}{\beta_F} & -c \frac{m_{bnt}}{\beta_F} \end{bmatrix},$$

$$\mathbf{x} = \begin{bmatrix} z \\ \dot{z} \\ p \\ \dot{p} \end{bmatrix}, \quad \mathbf{b}_F = \frac{\eta}{\beta_F r} \begin{bmatrix} 0 \\ m_n \\ 0 \\ m_{bnt} \end{bmatrix},$$

$$\mathbf{e}_F(\mathbf{x}) = \frac{1}{\beta_F} \begin{bmatrix} 0 \\ -\alpha(m_{bnt}g + f_{fF}) + \\ m_n(m_n g - \kappa(s_0 - l_0) - f_p) \\ 0 \\ -m_n f_{fF} - m_{bnt}(\kappa(s_0 - l_0) + f_a) \\ 0 \end{bmatrix}.$$

Notice that the actuator dynamics are important during flight. For any controller there is a minimum hopping height, below which it is not possible to servo the actuator length back to zero before the next touchdown occurs.

3.2 Motor Model

Our motors behave like ideal “torquer’s,” that is, we can control instantaneous current up to the thermal and operational limits imposed by the motor construction and the drive electronics. Since we operate intermittently we are able to draw the maximum stall torque of 1.78 Nm and utilize the operational regime for short term operation in the first quadrant given by the manufacturer (Figure 2).

We have adjusted the amplifier supply voltage to 40V to provide the motor’s stall torque of 1.78 Nm. The resulting operating regime is shown in Figure 3, which was obtained experimentally by commanding a desired torque square wave profile between +1.78 and -1.78 Nm. The motor torque is limited by

$$\tau \begin{cases} \leq \hat{\tau}(1 - \frac{\omega}{\omega_{max}}) & \text{First quadrant} \\ \leq \hat{\tau} & \text{Second quadrant} \\ \geq -\hat{\tau}(1 + \frac{\omega}{\omega_{max}}) & \text{Third quadrant} \\ \geq -\hat{\tau} & \text{Fourth quadrant} \end{cases} \quad (3)$$

for our motor and will be qualitatively limited in the same fashion for other motors in this class of fractional horsepower motors. It is therefore evident that the traditional actuator limits of the form

$$\|\tau\| \leq \hat{\tau}$$

is not applicable to this class of electric DC motor which is increasingly common for driving small to medium size robots and mechanisms.

4 Problem Formulation

Our hopper belongs to the class of intermittent dynamical systems. They are characterized by intermittent contact with an environment, with a resulting change of system dynamics. In addition, it is “underactuated,” possessing fewer actuated degrees of freedom (1) than motion degrees of freedom (2). We are currently building a planar hopper which

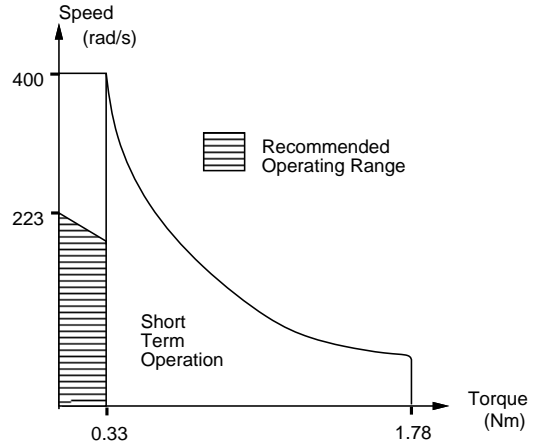


Figure 2: Torque speed curve of the Maxon Series 2260 brushed 80W DC motor, adapted from [1]

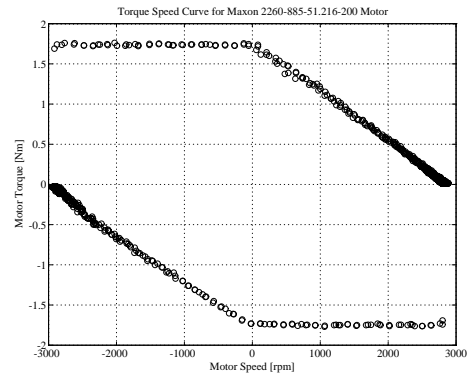


Figure 3: Experimental torque speed curve. Note that in the second and fourth quadrants we have artificially limited the motor torque command to $\hat{\tau}$ in order not to exceed the manufacturer’s specified maximum torque. Unless the actuator is back driven, all of the stance phase will occur in the first quadrant.

has five motion degrees of freedom, but only two actuated degrees of freedom. These two properties are common in legged robots and not only complicate control, but also render the traditional approach of encoding the task via reference trajectory unsuitable. In past research on robot juggling – also an intermittent dynamical task where a one degree of freedom robot controlled a two and a four degree of freedom environment [2] – a more parsimonious task encoding was found.

Instead of concerning ourselves with the continuous dynamics described in the previous section, we shall base the problem formulation on the discrete map between successive touchdown velocities,

$$w_{j+1} = f(w_j, \tau(t)), \quad (4)$$

where $w_j = [\dot{z}(t_j)^- \quad \dot{p}(t_j)^-]^T$ is the vector of body and actuator velocities just before touchdown, and $\tau(t)$ is the motor torque profile between the j^{th} and the $(j+1)^{\text{th}}$ touchdown. The robot control problem results from prescribing some desired sequence of robot touchdown velocities, $\{w_j^*\}$ and asking for a controller $\tau(t)$, subject to (3) which results in asymptotic convergence of w_j to w_j^* . The simplest hopper task is a constant w^* which encodes a constant hopping height.

5 Open Loop Control

Motivated by Raibert’s open loop controller for achieving a constant hopping height, which specifies a fixed actuator displacement at the lowest body height, we employ a new open loop continuous torque strategy during stance phase,

$$\tau = \bar{\tau} \left(1 - \frac{\omega}{\hat{\omega}}\right), \quad (5)$$

with $0 \leq \bar{\tau} < \hat{\tau}$ in the first quadrant (stance), and a simple high gain PD controller to return the actuator. This algorithm stabilizes our hopper, as will be shown in the following section. Note also, that this strategy is exactly implementable since it satisfies (3).

6 Simulation and Experimental Verification

In order to validate the model derived in Section 3, we now compare simulations with experiments. Most of the parameters shown in Figure 1 are known via direct measurement $(m_b, m_n, m_t, \kappa, s_0, l_0)$, or are known from manufacturer’s data (J, r) . Only the friction coefficients are left to identify. To this end, we compared experimental runs with simulations iteratively while modifying those constants. This simple parameter identification procedure will be improved in the near future with a more systematic identification process. We are also pursuing online parameter identification procedures which run concurrently with the robot controller.

The results of the parameter identification are listed in Table 1 and shown the corresponding plots of passive and active robot responses in Figure 4 and Figure 5, respectively. Both comparisons show close matching between the computer simulations based on the model from Section 3 and experiments. In addition, Figure 6 and Figure 7 show the total energy plots and their simulated counterparts from the same experimental runs.

Next, in Figure 8 the desired and actual motor torques are shown during two hopping cycles at steady state. The stance phases are the short time periods of about 0.15s indicated by the markers. First, we see that the actuator model is accurate, since the torque error is small, and we stay well within the allowable torque regime throughout the stance phases. Second, the torque magnitudes required for stable steady state hopping are well below the available peak torque of 1.78Nm. Torque requirements for transients and active control laws which we are going to implement in the near future should be readily satisfied. Finally, notice that at the beginning of the flight phase, a peak torque of 2.5Nm is commanded via the PD controller employed. However, sufficient flight time is available to servo back the leg with considerably less torque.

The low power requirements are shown in Figure 9. During stance, the average power requirement is only 80W, with a peak of 120W, well below the peak power available from our motor. The energy added by the motor to the system is docu-

mented in Figure 10, and reaches $12J$ by the end of stance phase. Unfortunately, of this amount, almost $4J$ are lost due to the current leg design, as is evident from the plot of elastic energy stored in the leg spring, Figure 11. Since liftoff and touchdown occur at the same height, $z_{lo} = z_{td}$, at liftoff the energy stored in the spring resulting from the actuator travel during stance, can not be recovered, and is dissipated during flight. We are currently changing the leg design to utilize this substantial amount of energy. Resulting in a net energy gain of 30%, this redesign will have a positive effect on the overall hopping energetics.

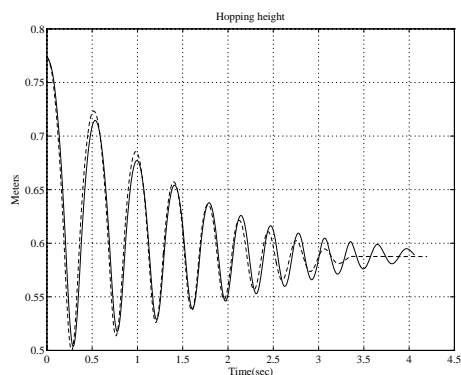


Figure 4: Comparison of unactuated hopper simulation with experiment

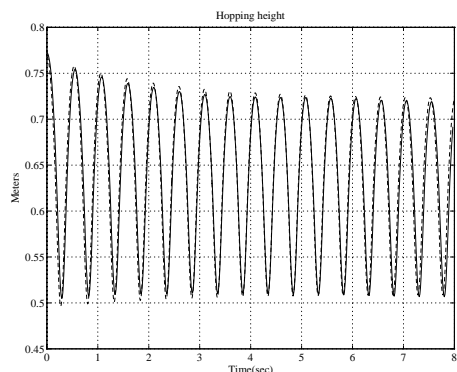


Figure 5: Comparison of actuated hopper simulation with experiment

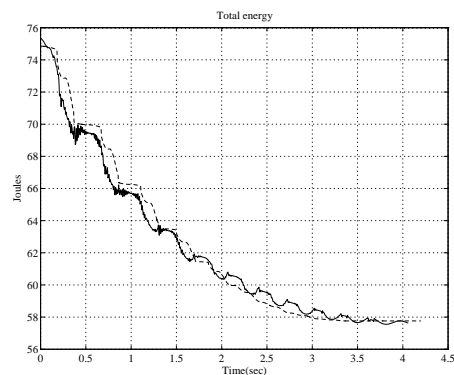


Figure 6: Comparison of unactuated hopper simulation with experiment

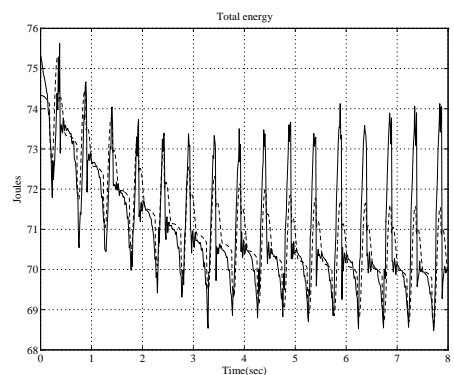


Figure 7: Comparison of actuated hopper simulation with experiment

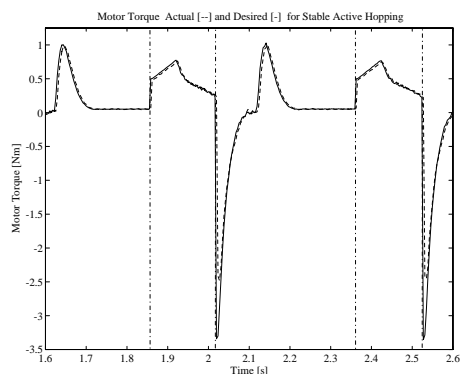


Figure 8: Experimental measurement of actual motor torque versus desired motor torque.

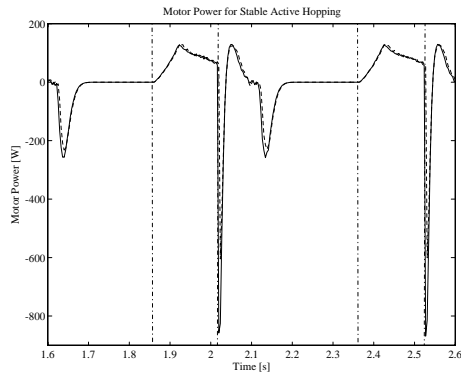


Figure 9: Experimental measurement of actual motor power versus desired motor power.

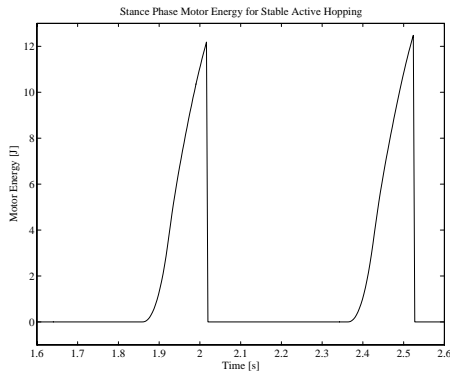


Figure 10: Experimental measurement of energy added during stance phase.

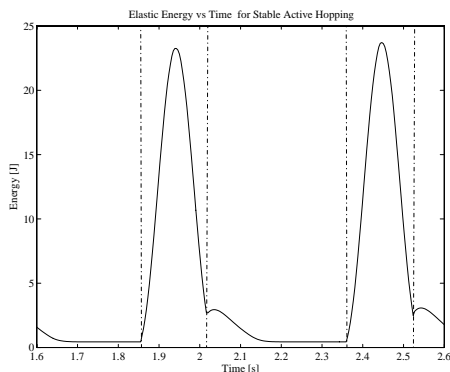


Figure 11: Experimental measurement of elastic energy during stable hopping.

Conclusion

This paper presented the current status of our work on model based control for dynamically stable legged robots. We presented a new robot leg design with electrical actuation, based on a highly efficient ball screw design. A dynamical model was derived which includes the actuator dynamics. The parameters were identified and the model was validated with respect to experimental data. These two contributions together already permit the beginning of a symbiotic link between theoretical analysis and experimentally successful robot control. Our next step for this vertical hopper is to synthesize and implement robust controllers and verify their global stability properties analytically. These controllers will then serve as the basis for our planar hopper.

In the long run, we plan to build fully dexterous and autonomous legged robots. Specifically we aim at the design and control of an autonomous quadruped with articulated legs, actuated by electric motors. Such a machine is a research tool, and our intent is to solve practical tasks via custom tailored derivatives of this machine. However, more research needs to be done in simpler settings, and we intend to follow Raibert's route of building successively more complex machines. In fact the present leg has been designed as part of a planar robot which we are currently building. This robot will let us study most of the fundamental dynamic legged locomotion problems common to all legged robots.

Acknowledgements

We thank Dan Koditschek for stimulating discussions and Marc Raibert for having made possible a post doc for the third author in 90/91, during which this work was motivated, and which generated the excitement for this field of research. We thank also M. Moghaddam for his planarizer design and general help with this project. This work has been supported in part by a Major Equipment Grant from the McGill Graduate Faculty, an Equipment Grant from the McGill Faculty of Graduate Studies and Research, and an NSERC/CIAR Junior Industrial Research Chair held by the third author. Support

for HR was provided by the Ministry of Culture and Higher Education of Iran, and for PG by an NSERC PGSA scholarship.

References

- [1] Interelectric AG. *Maxon Motor*. Sachseln, Switzerland, 91/92.
- [2] M. Buehler, D. E. Koditschek, and P. J. Kindlmann. Planning and Control of Robotic Juggling Tasks. In H. Miura and S. Arimoto, editors, *5. Int. Symp. Robotics Research*. MIT Press, 1990.
- [3] H. M. Hmam and D. A. Lawrence. Robustness analysis of nonlinear biped control laws via singular perturbation theory. In *Proc. IEEE Int. Conf. Decision and Control*, Tucson, AZ, Dec 1992.
- [4] J. M. Hollerbach, I. W. Hunter, and J. Ballantyne. A comparative analysis of actuator technologies for robotics. In O. Khatib, J. J. Craig, and T. Lozano-Perez, editors, *The Robotics Review 2*. MIT Press, Cambridge, MA, 1991.
- [5] I. W. Hunter and S. Lafontaine. A comparison of muscle with artificial actuators. *Proc. Sensors and Actuators*, 1992.
- [6] D. E. Koditschek and M. Buehler. Analysis of a Simplified Hopping Robot. *Int. J. Robotics Research*, 10(6), Dec 1991.
- [7] V. V. Lapshin. Vertical and horizontal motion control of a one-legged hopping machine. *Int. J. Robotics Research*, 11(5), 1992.
- [8] Z. Li and J. He. An energy perturbation approach to limit cycle analysis in legged locomotion systems. *Proc. IEEE Int. Conf. Decision and Control*, 1990.
- [9] K. V. Papantoniou. Electromechanical design for an electrically powered, actively balanced one leg planar robot. In *Proc. IEEE Conf. Intelligent Systems and Robots*, Osaka, Japan, 1991.
- [10] K. A. Pasch and W. P. Seering. On the drive systems for high-performance machines. *Transactions of the ASME*, 106, Mar 1984.
- [11] M. H. Raibert. Dynamic stability and resonance in a one-legged hopping machine. *4th Symp. Theory and Practice of Robots and Manipulators*, 1981.
- [12] M. H. Raibert. *Legged Robots That Balance*. MIT Press, Cambridge, MA, 1986.

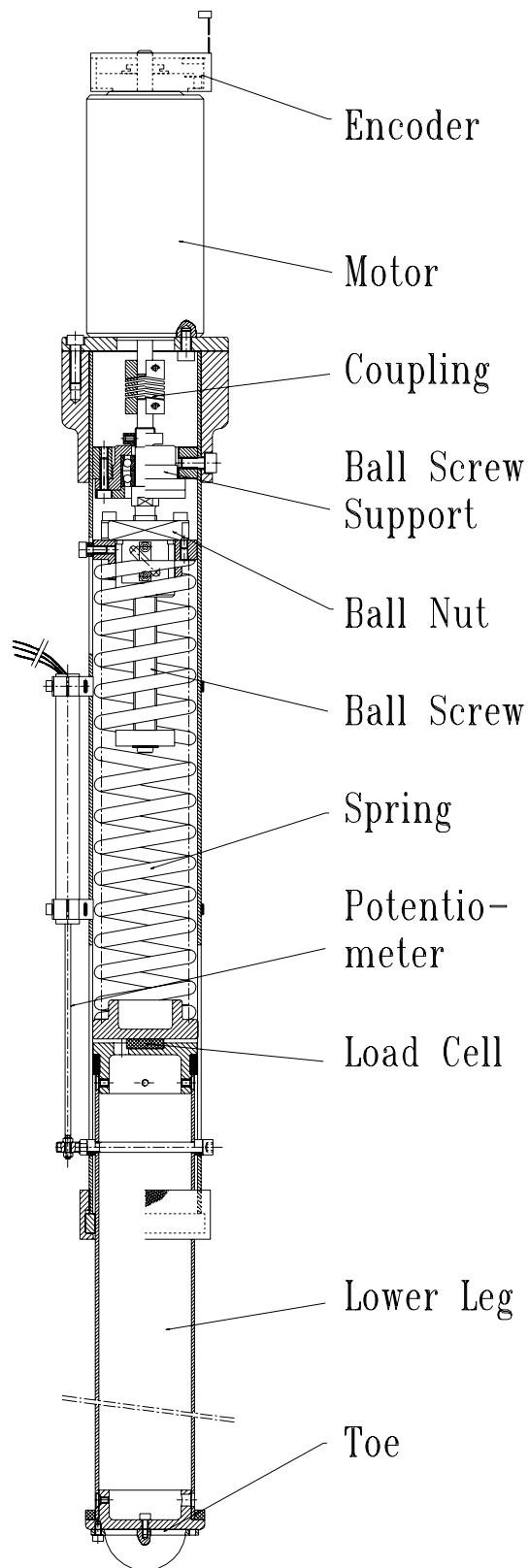


Figure 12: The Hopper, Assembly Drawing

- [13] A. F. Vakakis and J. W. Burdick. Chaotic motions of a simplified hopping robot. In *Proc. IEEE Int. Conf. Robotics and Automation*, Cincinnati, OH, 1990.

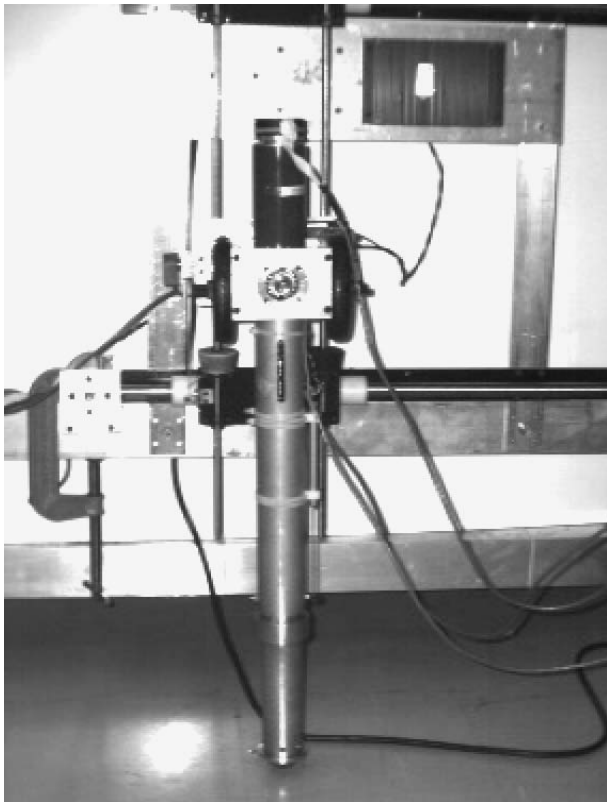


Figure 13: The Hopper